Comparison of three forecasting models for groundwater levels: a case study in the semiarid area of west Jilin Province, China

Zhao Ying, Lu Wenxi, Chu Haibo and Luo Jiannan

ABSTRACT

As groundwater is a critical source of water for both drinking and agriculture in Jilin Province, China, it is important to investigate and understand groundwater level dynamics in this area. Time-series analysis and artificial neural networks (ANN) are commonly used for analysing and forecasting groundwater levels. The integrated time-series (ITS) and auto-regressive integrated moving average (ARIMA) are the most commonly used models for time-series analysis. Among ANN approaches, the radial basis function neural network (RBFNN) is a widely used model for making empirical forecasts of hydrological variables. There are no previous reports comparing the ITS, ARIMA and RBFNN models together in groundwater-level dynamics literature. An attempt has been made in this study to investigate the applicability of these three models for the prediction of groundwater levels based on root mean squared error, the Nash-Sutcliffe coefficient and mean absolute error. The results indicated that all three models reproduced groundwater levels accurately. In addition, the RBFNN model was more reliable than ITS and ARIMA. This provides a choice in the selection of models for analysis and prediction of groundwater levels. The predicted results also provide a basis for rational exploitation and sustainable utilization of groundwater resources.

Key words | forecasting, groundwater level, Jilin Province, radial basis function neural networks, time-series analysis

Zhao Ying
Lu Wenxi (corresponding author)
Chu Haibo
Luo Jiannan
Key Laboratory of Groundwater Resources and Environment Ministry of Education,
Jilin University,
Changchun 130021,
China
E-mail: *luwenxi@jlu.edu.cn*

INTRODUCTION

Western Jilin Province, located in the northeast of China, is one of China's most important agricultural and livestock areas. With a semiarid continental climate, it is among the largest grain-producing provinces and is one of the regions designated for future crop expansion. The normal annual precipitation is about 400 mm, and the mean annual potential evapotranspiration for the study area is generally taken as 1,900 mm (Bian *et al.* 2012). Groundwater in the region is crucial for crop growth and production, and knowledge of the dynamics is necessary for ensuring a sustainable water resource. Many unauthorized wells are used in the region and pumping volume is not regulated, resulting in overexploitation of the aquifer and lowering of the water table over many years (Ma *et al.* 2012).

Although conceptual and physically based models are the main tools for depicting hydrological variables and understanding the physical processes taking place in such a system, they have their practical limitations. When insufficient data is available, and making accurate predictions is more important than understanding the physics, empirical models remain a reasonable alternative, providing useful results without taking up costly calibration time (Daliakopoulos *et al.* 2005; Nikolos *et al.* 2008). Time-series models and artificial neural network (ANN) models are such 'black box' models whose properties are ideally suited to dynamic system modelling.

Time-series models based on stochastic theory include the integrated time-series (ITS) model, the auto-regressive

doi: 10.2166/aqua.2014.023

moving average (ARMA) model, the auto-regressive integrated moving average (ARIMA) model, the seasonal auto-regressive moving average model and the periodic auto-regressive model (Ahn 2000; Wong *et al.* 2007; Yang *et al.* 2009). A major advantage of time-series models is that they are easy to use without requiring a great deal of other data, and the usefulness of their results can be accurately assessed.

ANN models have been used for groundwater level prediction (e.g. Krishna *et al.* 2008; Tsanis *et al.* 2008; Banerjee *et al.* 2009; Sreekanth *et al.* 2009; Sethi *et al.* 2010; Heesung *et al.* 2011; Yi *et al.* 2012; Mohanty *et al.* 2013), aquifer parameter determination (Samani *et al.* 2007; Karahan & Ayvaz 2008) and groundwater quality monitoring (Milot *et al.* 2002; Farmaki *et al.* 2013). An important feature of ANN models is their ability to detect patterns in complex systems (Adamowski & Chan 2011).

There have been a number of comparative studies including time-series models and ANN (Yang *et al.* 2009; Claveria & Torra 2014). They either compare ARIMA with ANN or contrast ITS with back propagation ANN. In the present study, the potential of two often-used time-series models (ITS and ARIMA) and the radial basis function neural network (RBFNN) model were evaluated for predicting groundwater levels. There are no previous reports in the groundwater-level dynamics literature that compare ITS, ARIMA and RBFNN models together. The aims of the present study were (1) to apply and compare the advantages and disadvantages of the three models for forecasting groundwater levels in areas where the water table has been steadily falling over the past decade due to overexploitation and (2) to provide reliable data on which to base reasonable exploitation that would ensure sustainable utilization of groundwater.

METHODOLOGY

Time-series analysis

ITS models

The principle of ITS models is to separate a time series into four major components (trend, seasonal, periodic and random), and then add these together to get the final forecasting model. The basic equation is

$$H_t = X_t + S_t + P_t + R_t \tag{1}$$

where H_t is the time series; X_t is the trend component; S_t is the seasonal component; P_t is the periodic component; and R_t is the random component.

In most published articles on this subject (e.g. Zhao *et al.* 2007; Zhou *et al.* 2007; Yang *et al.* 2009; Lu *et al.* 2012), time series are divided into three parts – trend, periodic and random components. The seasonal component S_t was added in the present study, as it reflects the influence of rainfall variation, which is an important consideration in the analysis of groundwater levels, particularly in the semiarid regions.

X_t stands for the general trend in a single series. It can be determined in many ways, including smoothing or polynomial fitting techniques. In this study, polynomial fitting was chosen because it is readily done in Excel software using the 'add trendline' tool.

S_t indicates how the series varies throughout the year and was found to be strongly correlated with rainfall. It was determined by a multi-year averaging method: after extracting the trend component, the series of $H_t - X_t$ is obtained; then the average value of $H_t - X_t$ is calculated for corresponding months in different years. From this, 12 weighting values – one for each month – were calculated. After determining the seasonal component, it was then removed, so that $H_t - X_t - S_t$ becomes the series to be analysed when determining the periodic component.

P_t, the periodic component, signals the interannual variability of the series. The harmonic wave analysis method of Olsson & Eklundh (1994) was used to determine its value. This method supposes that the periodic component should comprise many different cyclic waves, and therefore may be expressed as the Fourier series

$$\hat{P}_t = \frac{a_0}{2} + \sum_{k=1}^{L}\left[a_k \cos\frac{2pkt}{n} + b_k \sin\frac{2pkt}{n}\right] \tag{2}$$

where $\hat{P}_t$ is the estimated value of p_t; a_0 is the average of p_t; L is the magnitude of the waves; k is the number of waves;

a_k, b_k are coefficients; and n is the number of samples. After it has been calculated, the periodic component is removed. $H_t - X_t - S_t - P_t$ then becomes the series to be analysed when determining the random component.

R_t, the random component, is the last to be calculated. It is influenced by many uncertain factors, such as noise. It was extracted by the auto-regression method (Gemitzi & Stefanopoulos 2011)

$$\hat{R}_t = \Phi_0 + \Phi_1 r_{t-1} + \Phi_2 r_{t-2} + \ldots + \Phi_p r_{t-p} + e_t, \quad (3)$$

where p is the model order determined by the Akaike information criterion (AIC) and Φ_i is the autoregression coefficient. The p value is selected when the AIC(p) takes a minimum value from

$$AIC(p) = n \ln \hat{\sigma}_p^2 + 2p, \quad (4)$$

where n is the amount of data; $\hat{\sigma}_p^2$ is the variance of the residuals of AR(p); and e_t represents the residuals of evaluation (Akaike 1969).

ARIMA models

For more than half a century, ARIMA models have dominated many areas of time-series forecasting. In the ARIMA (p,d,q) model, the future value of a variable is assumed to be a linear extrapolation of several past observations and random errors. That is, the underlying process that generates the time series with a mean value μ has the form

$$\Phi(B)\nabla^d(y_t - \mu) = \theta(B)a_t \quad (5)$$

where y_t and a_t are the actual value and random error for the time period t, respectively; $\Phi(B) = 1 - \sum_{i=1}^{p} \varphi_i B^i$, $\theta(B) = 1 - \sum_{j=1}^{p} \theta_j B^j$, are polynomials in B of degree p and q; φ_i ($i = 1, 2, \ldots, p$) and θ_j ($j = 1, 2, \ldots, q$) are the model parameters; $\nabla = 1 - B$; B is the backward shift operator; p, q are the orders of the model; and d is the order of differencing. Random errors a_t are assumed to be independently and identically distributed with a mean of zero and a constant variance of δ^2.

Radial basis function neural networks

The RBFNN was proposed by Moody and Darken in the late 1980s and has been widely used for classification or function approximation since then (e.g. Chu *et al.* 2013). It mainly consists of three layers: an input layer, a hidden layer and an output layer. A single output RBFNN with K hidden layer neurons is expressed as:

$$y_k = \sum_{i=1}^{m} w_{ik} R_i(x) + \theta_k \quad (6)$$

where y_k is the kth output node on the output layer; ω_{ik} is the weight connection between ith hidden and kth output nodes; and θ_k is the threshold value of the kth output node.

The most commonly used function in the hidden layer is the Gaussian function, given by

$$R_i(x) = e\left[-\|x - c_i\|/2\sigma_i^2\right] \quad \mathrm{i} = 1, 2 \ldots, m \quad (7)$$

where x is the n-dimensional input vector; c_i is the centre of the ith radial basis function; σ_i is the spread of the radial basis function in the ith hidden node that indicates the radial distance from the RBF centre; m is the number of hidden nodes; and $\|x - c_i\|$ is the radial distance from X to the RBF centre.

The training process for RBFNN may be divided into two stages. The first is forward propagation, where data is processed from the input layer to the hidden layer and finally to the output layer. Through the calculations in every layer, the actual outputs were obtained. The second stage is reverse propagation of the error. The error between the network output and the actual value is calculated. If the error does not fall within a permissible value, the network weight and spread of the RBF are adjusted. The error is propagated backwards from the output layer to the hidden layer and then to the input layer. Forward and reverse propagation are performed in a single iteration, which is repeated until the error reaches its permissible value, or until the learning cycle time has elapsed.

The number of hidden neurons is found to have a large influence on the output of the RBF. The optimal number of hidden neurons is able to be identified by the root mean squared error (RMSE). When the RMSE drops to the

lowest point, the corresponding number is the optimal number of hidden neurons.

Criteria of evaluation

Three standard statistical measures, that is, RMSE, the Nash–Sutcliffe coefficient (NS) and mean absolute error (MAE), were used to evaluate the performances of the forecasting models. The RMSE evaluates the residual between observed and forecast values and NS evaluates the capability of the model to forecast groundwater level away from the mean. MAE is a measure of the difference between observed and forecast values. The closer the NS value is to 100, the more accurate the forecasting. The closer the RMSE and MAE values are to 0, the more accurate the forecasting. These are calculated from

$$\mathrm{RMSE} = \sqrt{\frac{\sum_{i=1}^{n} (f_i - F_i)^2}{n}}, \tag{8}$$

$$\mathrm{NS} = \left[1 - \frac{\sum_{i=1}^{n} (f_i - F_i)^2}{\sum_{i=1}^{n} (f_i - \bar{f}_i)^2}\right] \times 100 \tag{9}$$

$$\mathrm{MAE} = \frac{\sum_{i=1}^{n} (f_i - F_i)^2}{n} \tag{10}$$

where f is observed data; F is the predicted data; and $\bar{f}$ is the mean observed value.

STUDY AREA AND DATA DESCRIPTION

The three models were tested with data taken from the western part of Jilin Province, China (Figure 1). Two typical wells located in Baicheng City and Songyuan City were chosen because groundwater levels at those locations had declined in the recent decades due to overexploitation. The level was measured monthly from 1986 to 2013. The time series was divided in two data subsets, one for establishing the time-series models and training the neural network (1986–2005), the other for model validation (2006–2013).

MODELLING

ITS model

All tests and results were obtained by using MATLAB 2011b and Excel 2007 software. The trend component (Figure 2) showed that the depth of the water table fell yearly during that period. The groundwater depth should not increase or decrease continuously under natural (unexploited) conditions. It should be steady or variable within a certain range. Thus the trend component reflects the degree of exploitation of the water resource by residents.

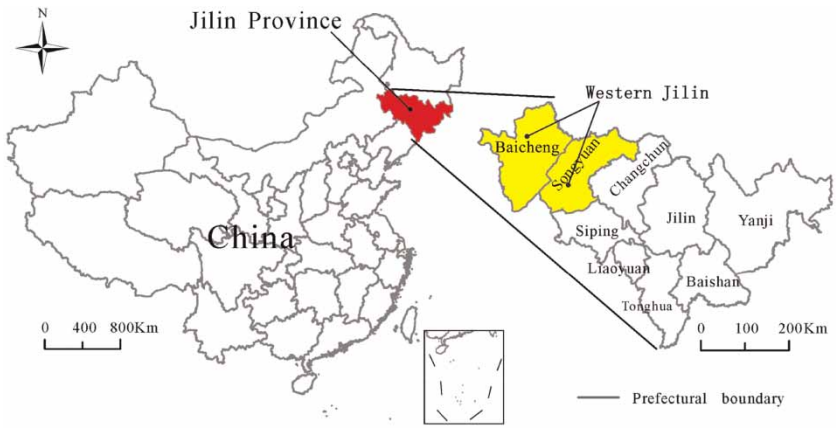

Figure 1 | Study area, western Jilin Province, China.

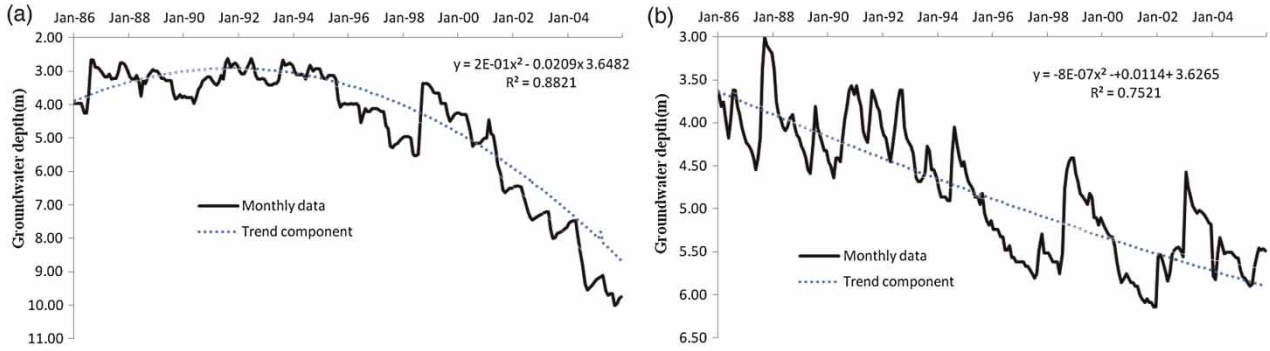

Figure 2 | Trend component for Baicheng (a) and Songyuan (b).

The seasonal component (Figure 3) was greater in January–June than July–December, consistent with the beginning of the rainy season in June. The rise in the water table was delayed because soil in the unsaturated zone absorbs water at the beginning of the rains. As a consequence, the water table began to rise in July. When the rainy season ended, the level dropped to its former state. Thus, the seasonal component implies the fluctuation of groundwater level influenced by rainfall.

From the periodic component (Figure 4), it can be seen that the groundwater levels at both locations had a 7- to 9-year periodicity. Almost three complete cycles were distinguished in the 19-year period from 1986 to 2005. The periodicity is believed to be driven by the cycle of solar activity and the Earth's rotation and revolution (Zheng 1989). Sunspot activity is thought to influence the alternation of the rainy and dry seasons. The periodicity reflects the influence of natural climatic factors, and is also believed to be driven by the periodicity of rainfall (Hao *et al.* 2012). In the present study, the hydrological environment was karst, in which the interrelationship of surface and subsurface is strong, but for porous media, and the effect of unsaturated zones, the relationship may be not as obvious. In addition, the periodicity of precipitation in western Jilin Province is 2, 11 and 30 years (Wang *et al.* 2011). What is more, solar activity and the Earth's rotation are also thought to influence rainfall, so the driving forces still need further study.

The random component (Figure 5) is influenced by many uncertain factors such as earthquakes and is not discussed further in this study. The fitted graphs are shown in Figure 6.

ARIMA model

The historical data indicated that groundwater depth was a non-stationary sequence. For a non-stationary time series,

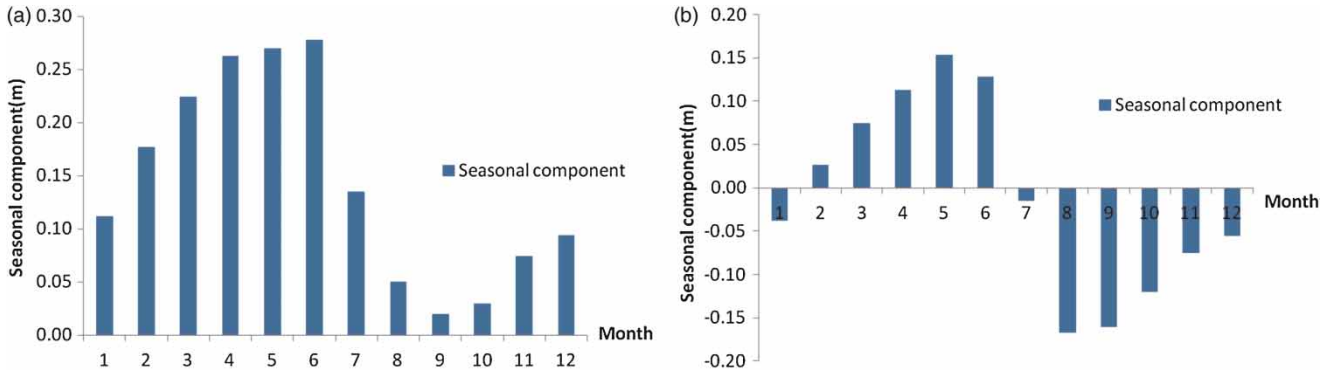

Figure 3 | Seasonal component for Baicheng (a) and Songyuan (b).

Figure 4 | Periodic component for Baicheng (a) and Songyuan (b).

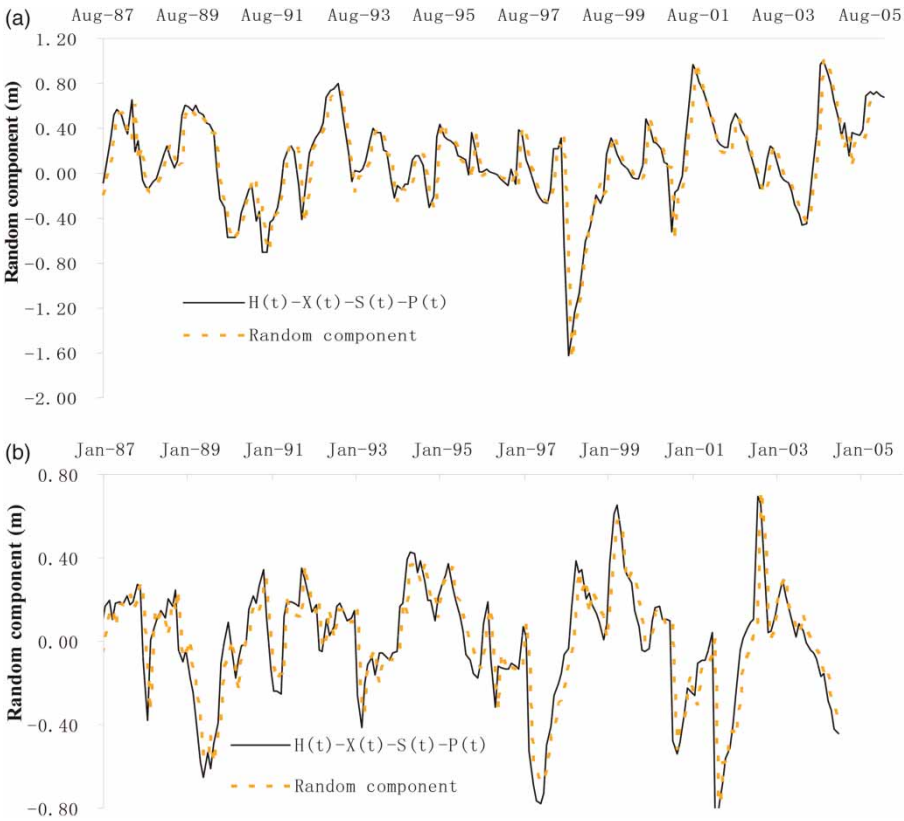

Figure 5 | Random component for Baicheng (a) and Songyuan (b).

(a)

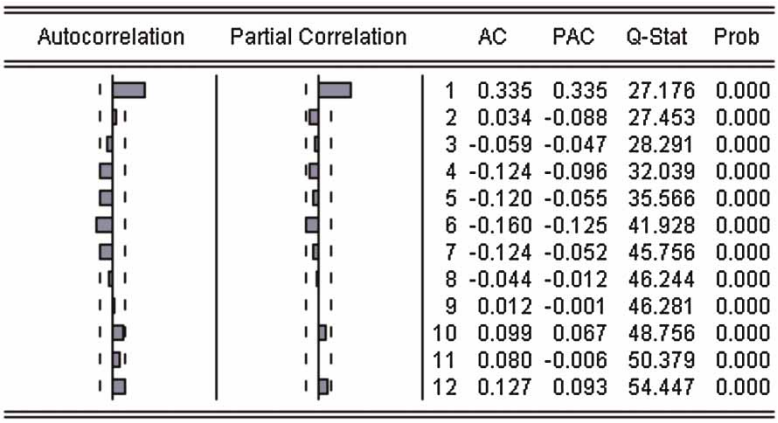

Autocorrelation	Partial Correlation		AC	PAC	Q-Stat	Prob
		1	0.335	0.335	27.176	0.000
		2	0.034	-0.088	27.453	0.000
		3	-0.059	-0.047	28.291	0.000
		4	-0.124	-0.096	32.039	0.000
		5	-0.120	-0.055	35.566	0.000
		6	-0.160	-0.125	41.928	0.000
		7	-0.124	-0.052	45.756	0.000
		8	-0.044	-0.012	46.244	0.000
		9	0.012	-0.001	46.281	0.000
		10	0.099	0.067	48.756	0.000
		11	0.080	-0.006	50.379	0.000
		12	0.127	0.093	54.447	0.000

(b)

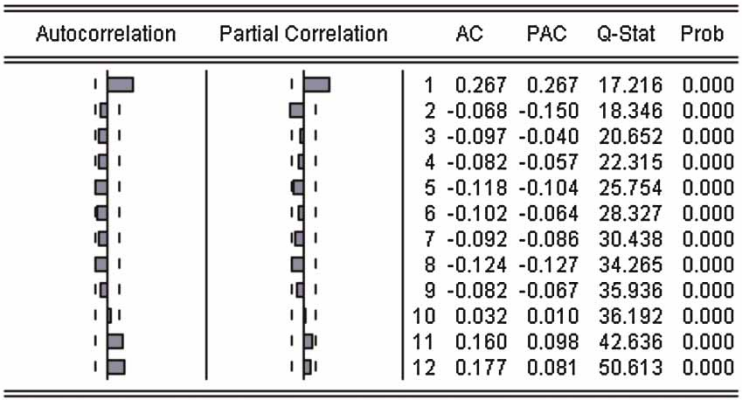

Autocorrelation	Partial Correlation		AC	PAC	Q-Stat	Prob
		1	0.267	0.267	17.216	0.000
		2	-0.068	-0.150	18.346	0.000
		3	-0.097	-0.040	20.652	0.000
		4	-0.082	-0.057	22.315	0.000
		5	-0.118	-0.104	25.754	0.000
		6	-0.102	-0.064	28.327	0.000
		7	-0.092	-0.086	30.438	0.000
		8	-0.124	-0.127	34.265	0.000
		9	-0.082	-0.067	35.936	0.000
		10	0.032	0.010	36.192	0.000
		11	0.160	0.098	42.636	0.000
		12	0.177	0.081	50.613	0.000

Figure 6 | Time-series correlation diagram for Baicheng (a) and Songyuan (b).

the differential makes it stationary, in effect. Using the augmented Dickey–Fuller unit root test, the order of differencing exponent, d, was fixed at 1; that is, $d = 1$ in the methodology of the ARIMA (p,d,q) model (see Equation (5)). Then the values of p and q were calibrated. From autocorrelation and partial correlation, the correlation diagram in Figure 6 was drawn. The default model was chosen as ARIMA (1,1,1). The calibrated parameters are shown in Table 1 and the corresponding fitted graphs in Figure 7.

RBFNN model

All test results were obtained using MATLAB 2011b software. The optimum network and parameter configuration were then derived by trial and error. The number of hidden neurons was found to have a large influence on the output of the radial basis function. The optimal number of hidden neurons was able to be identified by the RMSE. Figure 8 shows the effect on the network accuracy of changing the number of hidden neurons from 2 to 12. The training errors (RMSE) were minimal when four hidden neurons were modelled for Baicheng, and three for Songyuan.

Accordingly, for Songyuan, the three-layer RBFNN model contained eight neurons in the input layer, three in the hidden layer and one in the output layer; the spread of the Gaussian function was 20. For the Baicheng model, the model contained eight neurons in the input layer, four in the hidden layer and one in the output layer; the spread of the Gaussian function was 50.

Figure 8 shows the performance of the ITS and AR models in the process of establishing models and the fitting of the RBFNN model in the process of training the network. It is clear that the three models simulated the observations adequately, and consequently the performance of all three was evaluated.

Table 1 | Calibrated parameters for Baicheng and Songyuan

Variable	Coefficient	Standard error	*t*-statistic	Probability
Baicheng				
AR(1)	1.005025	0.003533	284.4735	0.0000
MA(1)	0.342756	0.061077	5.611857	0.0000
R^2	0.989533	Mean dependent variable		4.659205
Adjusted R^2	0.989489	SD dependent variable		2.001513
Standard error of regression	0.205206	AIC		−0.321270
Residual sum of squares	9.979972	Schwarz criterion		−0.292178
Log likelihood	40.39174	Hannah–Quinn criterion		−0.309547
Durbin–Watson statistic	1.971301			
Songyuan				
AR(1)	1.000484	0.002914	343.2963	0.0000
MA(1)	0.317003	0.061588	5.147190	0.0000
R^2	0.950668	Mean dependent variable		4.829791
Adjusted R^2	0.950460	SD dependent variable		0.7504939
Std error of regression	0.167030	AIC		−0.732953
Residual sum of squares	6.612070	Schwarz criterion		−0.703862
Log likelihood	89.58792	Hannah–Quinn criterion		−0.721230
Durbin–Watson statistic	2.016551			

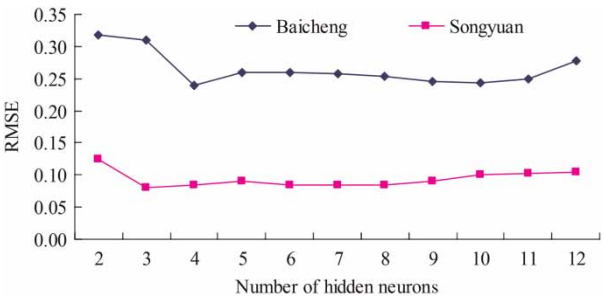

Figure 7 | RMSE sensitivity to the number of hidden neurons.

RESULTS AND DISCUSSION

Figure 9 and Table 2 summarize the results of validation of the three methods by the RMSE, NS and MAE. 'Short-term' and 'long-term' validations mainly refer to 1-year and 8-year validations. The comparisons show whether or not long-term prediction was acceptable in this study (Yang *et al.* 2009; Shiri *et al.* 2013).

It can be seen in Figure 10 that all three models were capable of predicting groundwater levels in the short term, but the ARIMA model was not effective in making long-term predictions. The RBFNN method demonstrated the closest agreement with observation, followed by the ITS and ARIMA models.

The same conclusion may be drawn from the information in Table 2. The RBFNN model has smaller RMSE and MAE and larger NS than the ITS and ARIMA models.

For both the 1-year and 8-year validations, a different result is seen for ITS and ARIMA. Validation accuracies of two models were almost identical for 1-year validation; however, significant differences exist for 8-year validation. For example, for Baicheng (Table 2) the RMSE, which evaluates the residual between observed data and model predictions, was respectively 0.20 and 0.19 for the 1-year validation of ITS and ARIMA. The NS, which indicates the deviation of the prediction from the mean, was 97 and 99 respectively

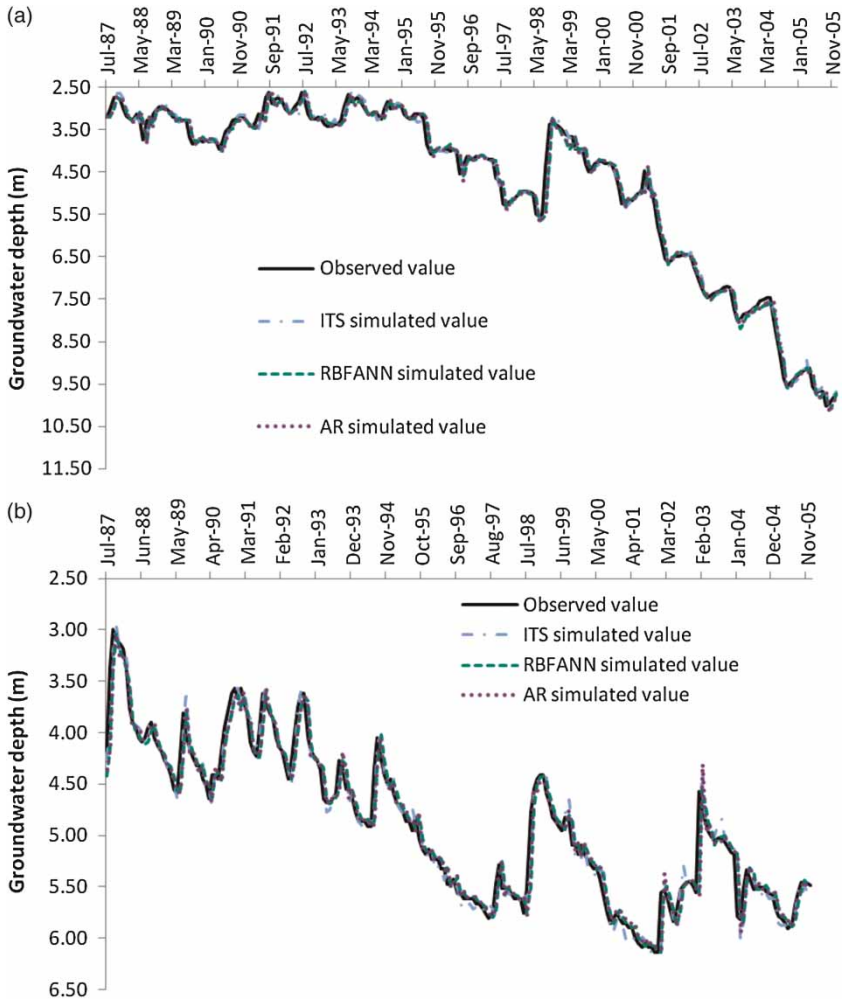

Figure 8 | Fitting graphs for Baicheng (a) and Songyuan (b).

for ITS and ARIMA. The MAE, which evaluates the difference between observed and predicted values, was respectively 0.15 and 0.12 for the ITS and ARIMA models. For 8-year validation, the ITS model was much more accurate than the ARIMA model. For example, for Baicheng (Table 2) the RMSE was 0.58 for the ITS model and 310 for the ARIMA model. The NS was 93 and 0.14, and the MAE was 0.47 and 89, respectively.

These results are consistent with those of Yang *et al.* (2009) in that the RBFNN model is better suited than ITS for predicting groundwater levels although the comparative accuracies of the three-component ITS model in Yang *et al.* (2009) and the four-component ITS model in the present study cannot be definitely stated because different data was used in the two cases. The performance of each criterion in the Baicheng region was poorer than in Songyuan because the groundwater depth data for Baicheng indicated much stronger variation than for Songyuan. Added to that, the variation of groundwater depth quoted in Yang *et al.* (2009) lay somewhere between that of Baicheng and Songyuan. As a result of these considerations, the same data for three- and four-component models will be assessed in a further study; nevertheless, incorporating the fourth (seasonal) component in the present work has undoubtedly aided the analysis of groundwater level variation.

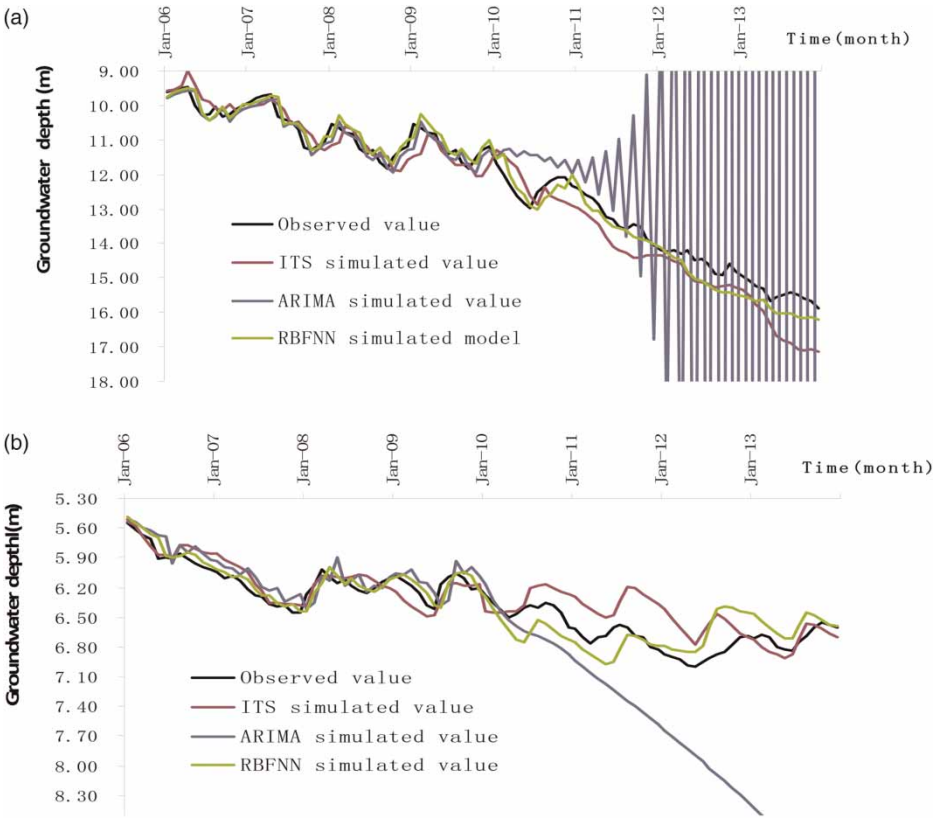

Figure 9 | Comparison of validation results with observed values for the different models for Baicheng (a) and Songyuan (b).

Table 2 | RMSE, NS and MAE goodness-of-fit criteria for the three models for Baicheng and Songyuan

	ITS		ARIMA		RBFNN	
Criterion	**1-year validation**	**8-year validation**	**1-year validation**	**8-year validation**	**1-year validation**	**8-year validation**
Baicheng						
RMSE	0.20	0.58	0.19	310	0.18	0.33
NS	97	93	99	0.14	99	99
MAE	0.15	0.47	0.12	89	0.12	0.27
Songyuan						
RMSE	0.10	0.19	0.12	0.9	0.07	0.15
NS	99	99	99	98	99	99
MAE	0.09	0.14	0.11	0.56	0.05	0.11

In general, the RBFNN model is suited to non-linear dynamic systems, whereas the other two models are more suited to linear dynamic systems. However, groundwater level variation is quite complex, and a non-linear analysis may be the better of the two. Although it is recognized that time-series analysis has its limitations, it also has its advantages; for instance, it reflects the influence of human activity, rainfall and solar fluctuation.

For forecasting the dynamics of the groundwater level, the RBFNN method is preferable, but for analysing

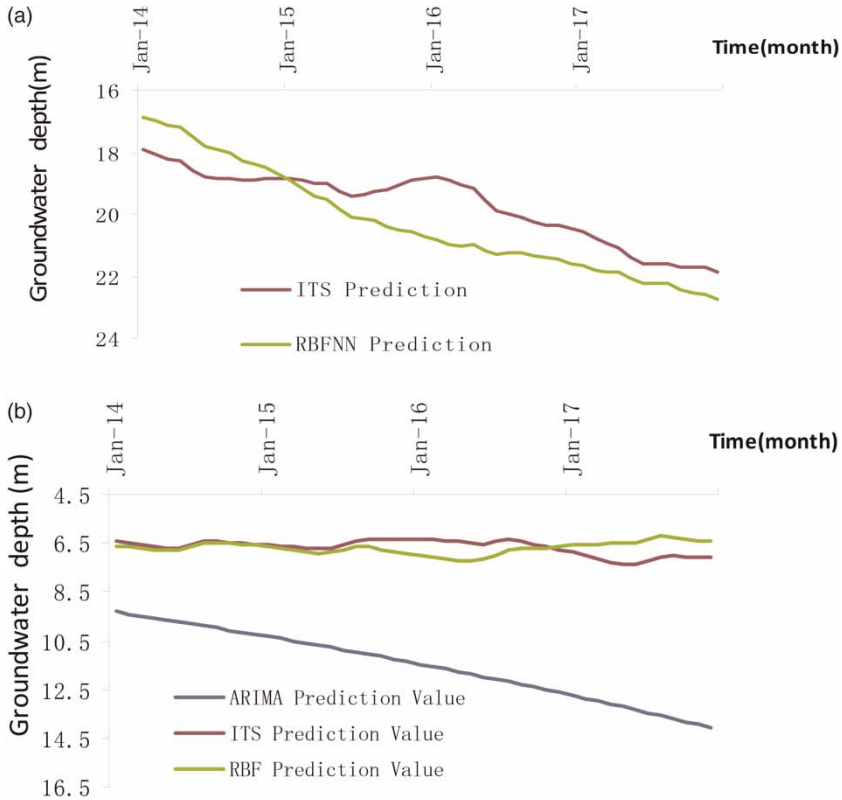

Figure 10 | Predicted results for (a) Baicheng and (b) Songyuan.

groundwater level variation, time-series analysis may be more appropriate. However, as expected, the efficiency of all three methods decayed as the prediction period increased. The results in Table 1 show that the 1-year validation was much superior to the 8-year validation; for the latter, the accuracy of the time-series analysis was relatively low. For long-term prediction, time-series analysis is not recommended compared with RBFNN.

PREDICTION

Three models were used to predict the groundwater level for the four years following the original experiment (i.e. 2014–2017). The results are shown in Figure 10. For Baicheng, because of the rapid groundwater variation, the ARIMA model was not capable of such a long-term forecast, so Figure 10(a) shows only the ITS and RBFNN forecasts. The results predict that the water table in Baicheng will continue to fall at the rate of 1 m/year if the present degree of exploitation continues. Figure 10(b) shows small predicted changes in the depth of the water table in Songyuan, remaining at an average depth of 6.5 m.

From the results of this study, it is clear that the ARIMA model was unsuitable for long-term groundwater level prediction and should not be used for this purpose.

CONCLUSIONS

All three models accurately simulated the observed groundwater data. The RBFNN model produced the most accurate simulations, especially in long-term predictions, and it is concluded that the RBFNN model was much more reliable than ITS and ARIMA for this purpose.

Despite its greater reliability, the RBFNN model has limitations that should not be overlooked. Conversely, the ITS and ARIMA models have certain advantages; for example, the ITS model is more applicable to the analysis of the factors that regulate groundwater dynamics: the trend, season and periodicity components reflect the degree

of water exploitation, rainfall, solar activity and the Earth's rotation and revolution around the Sun. The main advantages of the ARIMA model are the ease of calibrating its model parameters, and it is a sound choice for short-term prediction.

From the above results, it is recommended that groundwater exploitation in Baicheng be monitored in view of the continuous lowering of the water table over many years. As the predictions were all based on historical groundwater level measurement data, they all have certain limitations. If more relevant data were obtained, including rainfall data, knowledge of the relationship between the various factors would be improved.

ACKNOWLEDGEMENTS

This study is based on the work supported by the National Natural Science Foundation of China (41372237), National Water Pollution Control and Management of Science and Technology Major Projects (2012ZX07201), Doctoral Program of the Ministry of Education (20120061110058) and Project 2014025 supported by the Graduate Innovation Fund of Jilin University. The authors thank the editor and anonymous reviewers for their constructive comments and suggested revisions.

REFERENCES

Adamowski, J. & Chan, H. F. 2011 A wavelet neural network conjunction model for groundwater level forecasting. *J. Hydrol.* **407**, 28–40.

Ahn, H. 2000 Modeling of groundwater heads based on second-order difference time series models. *J. Hydrol.* **234**, 82–94.

Akaike, H. 1969 Fitting autoregressive models for prediction. *Ann I Stat. Math.* **21**, 243–247.

Banerjee, P. R., Prasad, K. & Singh, V. S. 2009 Forecasting of groundwater level in hard rock region using artificial neural network. *Environ. Geol.* **58**, 1239–1246.

Bian, J. M., Tang, J., Zhang, L. S., Ma, H. Y. & Zhao, J. 2012 Arsenic distribution and geological factors in the western Jilin province, China. *J. Geochem. Explor.* **112**, 347–356.

Chu, H. B., Lu, W. X. & Zhang, L. 2013 Application of artificial neural network in environment water quality assessment. *J. Agric. Sci. Technol.* **15**, 343–356.

Claveria, O. & Torra, S. 2014 Forecasting tourism demand to Catalonia: Neural networks vs. time series models. *Econ. Model.* **36**, 220–228.

Daliakopoulos, I. N., Coulibaly, P. & Tsanis, I. K. 2005 Groundwater level forecasting using artificial neural networks. *J. Hydrol.* **309**, 229–240.

Farmaki, E. G., Thomaidis, N. S., Simeonov, V. & Efstathiou, C. E. 2013 Comparative use of artificial neural networks for the quality assessment of the water reservoirs of Athens. *J. Water Supply Res. T.* **62**, 296–308.

Gemitzi, A. & Stefanopoulos, K. 2011 Evaluation of the effects of climate and man intervention on ground waters and their dependent ecosystems using time series analysis. *J. Hydrol.* **403**, 130–140.

Hao, Y. H., Liu, G. L., Li, H. M., Li, Z., Zhao, J. & Yeh, T.-C. J. 2012 Investigation of karstic hydrological processes of Niangziguan Springs (North China) using wavelet analysis. *Hydrol. Process.* **26**, 3062–3069.

Heesung, Y., Jun, S. C., Hyun, Y., Bae, G. O. & Lee, K.-K. 2011 A comparative study of artificial neural networks and support vector machines for predicting groundwater levels in a coastal aquifer. *J. Hydrol.* **396**, 128–138.

Karahan, H. & Ayvaz, M. 2008 Simultaneous parameter identification of a heterogeneous aquifer system using artificial neural networks. *Hydrogeol. J.* **16**, 817–827.

Krishna, B., Rao, Y. R. S. & Vijaya, T. 2008 Modeling groundwater levels in an urban coastal aquifer using artificial neural networks. *Hydrol. Process.* **22**, 1180–1188.

Lu, W. X., Yang, L. L., Gong, L., Yin, J. H. & Chu, H. B. 2012 Dynamic forecasting of groundwater table based on the improved time series analysis method: a case study of Huadian City, Jilin Province, China. *J. Jilin University (Earth Science Edn)* **42**, 367–372.

Ma, L., Wei, X. M., Bao, A. M. & Wang, S. F. 2012 Simulation of groundwater table dynamics based on Feflow in the Minqin Basin, China. *J. Arid Land* **4**, 123–131.

Milot, J., Rodriguez, M. J. & Serodes, J. B. 2002 Contribution of neural networks for modeling trihalomethanes occurrence in drinking water. *J. Water Res. Pl. ASCE* **128**, 370–376.

Mohanty, S., Jha, M. K., Kumar, A. & Panda, D. K. 2013 Comparative evaluation of numerical model and artificial neural network for simulating groundwater flow in Kathajodi–Surua Inter-basin of Odisha, India. *J. Hydrol.* **495**, 38–51.

Nikolos, I. K., Stergiadi, M., Papadopoulou, M. P. & Karatzas, G. P. 2008 Artificial neural networks as an alternative approach to groundwater numerical modeling and environmental design. *Hydrol. Processes* **22**, 3337–3348.

Olsson, L. & Eklundh, L. 1994 Fourier series for analysis of temporal sequences of satellite sensor imagery. *Int. J. Remote Sens.* **15**, 3735–3741.

Samani, N., Gohri-Moghadam, M. & Safavi, A. A. 2007 A simple neural network model for the determination of aquifer parameters. *J. Hydrol.* **340**, 1–11.

Sethi, R. R., Kumar, A., Sharma, S. P. & Verma, H. C. 2010 Prediction of water table depth in a hard rock basin by using artificial neural network. *Int. J. Water Res. Environ. Eng.* **2**, 95–102.

Shiri, J., Kisi, O., Yoon, H., Lee, K.-K. & Nazemi, A. H. 2013 Predicting groundwater level fluctuations with meteorological

effect implications – A comparative study among soft computing techniques. *Comput. Geosci.* **56**, 32–44.

Sreekanth, P. D., Geethanjali, N., Sreedevi, P. D., Ahmed, S., Ravi Kumar, N. & Kamala Jayanthi, P. D. 2009 Forecasting groundwater level using artificial neural networks. *Curr. Sci.* **96**, 933–939.

Tsanis, I. K., Coulibay, P. & Daliakopoulos, N. 2008 Improving groundwater level forecasting with a feedforward neural network and linearly regressed projected precipitation. *J. Hydroinform.* **10**, 317–330.

Wang, X. H., Lu, W. X., Gong, L. & Zhang, L. 2011 Features analysis of 54-years precipitation change in Tongyu city. *Water Res. Power* **29**, 1–3 (in Chinese).

Wong, H., Ip, W. C., Zhang, R. Q. & Xia, J. 2007 Non-parametric time series models for hydrological forecasting. *J. Hydrol.* **332**, 337–347.

Yang, Z. P., Lu, W. X., Long, Y. Q. & Li, P. 2009 Application and comparison of two prediction models for groundwater levels: a case study in Western Jilin Province, China. *J. Arid Environ.* **73**, 487–492.

Yi, Q. X., Bao, A. M., Luo, Y. & Zhao, J. 2012 Measuring cotton water status using water-related vegetation indices at leaf and canopy levels. *J. Arid Land* **4**, 310–319.

Zhao, J., Bu, Y. M. & Zhou, X. J. 2007 Application of time series analysis method in groundwater level dynamic forecast of Shenyang City. *Water Res. Hydropower Northeast* **277**, 35–37 (in Chinese).

Zheng, D. W. 1989 Time series analysis and studies of earth rotation. *Prog. Astron.* **7**, 118–124 (in Chinese).

Zhou, X. J., Lan, S. S. & Wang, B. 2007 Application of time series analysis in groundwater level forecast of Siping region. *Water Res. Hydropower Northeast* **277**, 31–34 (in Chinese).

First received 17 February 2014; accepted in revised form 8 May 2014. Available online 19 June 2014